Pion-nucleus single charge exchange induced by stopped negative pions

R. Nair, H. S. Plendl, and E. P. Gavathas
Florida State University, Tallahassee, Florida 32306

L.-C. Liu, R. J. Estep, B. J. Dropesky, J. D. Bowman, and J. N. Knudson
Los Alamos National Laboratory, Los Alamos, New Mexico 87545

B. J. Lieb
George Mason University, Fairfax, Virginia 22030

C. E. Stronach
Virginia State University, Petersburg, Virginia 23806

H. O. Funsten and J. Mackenzie
College of William and Mary, Williamsburg, Virginia 23185

(Received 19 December 1994; revised manuscript received 2 October 1995)

The branching ratio (BR) for stopped negative pion induced single charge exchange was experimentally determined for CH_2, ^{27}Al, ^{31}P, ^{32}S, ^{45}Sc, and ^{115}In. The BR for CH_2 agrees with a previous determination; the others can be understood in terms of the shell model structure of the targets. These results will facilitate studies of the effective pion-nucleon isovector interaction in nuclei at threshold energies.

PACS number(s): 25.80.Gn, 13.75.Gx

Nuclear single charge exchange (SCX) induced by stopped negative pions can provide information on isovector pion-nucleon (πN) interactions in the nuclear medium at threshold energies. With that information, one can set stringent constraints on the effective isovector πN amplitude needed for low-energy pion-nucleus optical models. It is worth noting that the investigation of such SCX reactions near threshold is complementary to studies of pionic atom formation, where the isoscalar πN interaction plays a dominant role.

In the present experiment, we have determined the branching ratio (BR) for π^--induced SCX close to threshold on selected targets. Because of the dominance of the pion absorption channel at this low energy and other experimental problems, only a few attempts to measure this BR have been reported in the literature. One such attempt resulted in upper limits for seven targets from $A=6$ to 208 [1]. In other experiments, BR values on five targets from $A=2$ to 27 and estimates on four more targets from $A=47$ to 408 were obtained [2,3].

We used a 50 MeV π^- beam from the low-energy pion channel at LAMPF. The pions were slowed down to 4 ± 1 MeV in a graphite degrader, so that they came to a complete stop in the target (Fig. 1). The beam contained 40% π^-, about 50% e^-, and about 10% μ^- [4]. The π^0's were detected with the LAMPF π^0 spectrometer described in Ref. [5]. The two photons emitted in the π^0 decay were detected in coincidence in the two spectrometer arms. Each arm contained a thin scintillator counter to veto charged particle events, three conversion planes, and an array of total-absorption Pb-glass blocks. Each conversion plane consisted of an active Pb-glass converter, three multiwire proportional chamber (MWPC) planes, and a trigger scintillator. When a photon converted in one of the three planes, the conversion coordinates were determined from the MWPC information, and the energy deposited in the converters and in the glass blocks which contained the full shower was measured. The total π^0 energy was calculated from the opening angle between the decay photons and the asymmetry between the energies deposited in each arm. The spectrometer was set with the γ-γ opening angle between the two arms in the horizontal plane. That angle was set at 162° as required by the kinetic energy of the π^0 in the laboratory system, which

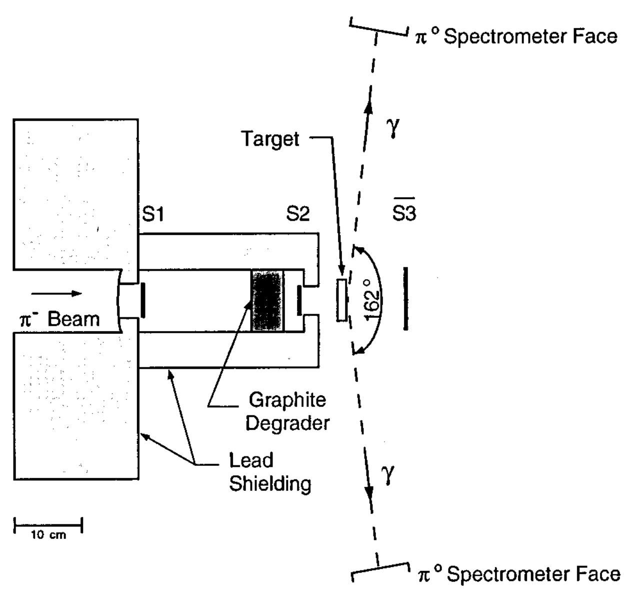

FIG. 1. Schematic top view of experimental setup. Scintillators $S1$ and $S2$ define the beam. To avoid background counts from the H content of the scintillators, $S2$ was housed inside a Pb collimator and the veto counter $\overline{S3}$ was removed during data collection.

TABLE I. Branching ratios of (π^-, π^0) reactions near threshold.

Target nucleus	(π^-,π^0) Q value (MeV)	No. of (π^-,π^0) events	Branching ratio $(\times 10^{-5})$
^{12}C	−9.31	0	0
CH_2	3.3	950	869±78
^{27}Al	1.42	3	<0.43
^{31}P	2.51	174	4.79±1.29
^{32}S	2.28	127	19.4±6.2
^{45}Sc	3.66	45	4.70±2.44
^{115}In	2.90	1	<0.21

varied from 1.33 to 3.66 MeV, depending on the reaction Q value (see Table I).

Targets of ^{31}P, ^{32}S, and ^{45}Sc were chosen for the expected relatively high BR for SCX, arising from the good overlap between the nuclear wave functions of the initial and final nuclei. Targets of ^{27}Al and ^{115}In were chosen for the expected small BR that results from the mismatch of the initial and final nuclear wave functions. Two other targets, ^{1}H and ^{12}C, were employed to check our measurements. The ^{1}H target (in the form of CH_2) was chosen because a large BR was expected, the ^{12}C target (in the form of graphite) because energy conservation forbids SCX near threshold. The targets of ^{27}Al, ^{45}Sc, and ^{115}In were self-supporting metal targets. The ^{31}P and ^{32}S targets were in pressed form. All targets were made just thick enough to stop the negative pions.

The number N_{π^-} of π^-'s that come to rest in the target was determined before and after each data run with the scintillator combination $S1$-$S2$-$\overline{S3}$ (Fig. 1). Typical rates were of the order of 10^5 π^-/s. During the data runs, the anticoincidence counter $\overline{S3}$ was removed to avoid π^0 background from the hydrogen content of the scintillator. The relative beam intensity during each data run was monitored with a toroidal current monitor through which the primary proton beam passed. The absolute normalization of the pion intensity was established before and after each data run by measuring the ^{11}C activity induced in scintillator disks. Although the cross section for $^{12}\mathrm{C}(\pi^-,\pi N)^{11}\mathrm{C}$ has been measured down to the energy with which the pions enter the degrader [6], it is not known at the lower energy with which the pions leave the degrader. Hence the activation measurements were made directly in front of it. The uncertainty in the beam flux determination, which included errors due to π^-'s either decaying in flight between $S2$ and the target or leaving $S2$ at such a large angle that they missed the target, varied with the target size from 8.5% for CH_2 to 12.5% for ^{45}Sc. Knowledge of the π^- flux was sufficient to normalize the experiment, because the μ^-/e^- contamination could not produce π^0's.

The number of π^0's produced, N_{π^0}, and the π^0 energy spectrum were determined in one or more data runs on each target. The CH_2 target was run for periods of 1 h, the others for periods of 3–30 h, depending on the yield. Target-out runs showed that there was no background due to π^-'s reacting in the air in front of the target. Appropriate shielding prevented background events from in-flight π^-'s that reacted in the components of the setup. Neutrons from $(\pi^-,2n)$ reactions could not produce a background, because such neutrons produce signals that are below the threshold of the spectrometer arm calorimeters. Contributions to the SCX yield from those π^-'s that enter the target with finite energy and interact before they are completely stopped are expected to be small, because the known experimental (π^-,π^0) cross sections decrease rapidly with incident pion energies. Corrections for such contributions cannot be made because severe experimental difficulties prevent (π^-,π^0) cross section measurements below 20 MeV.

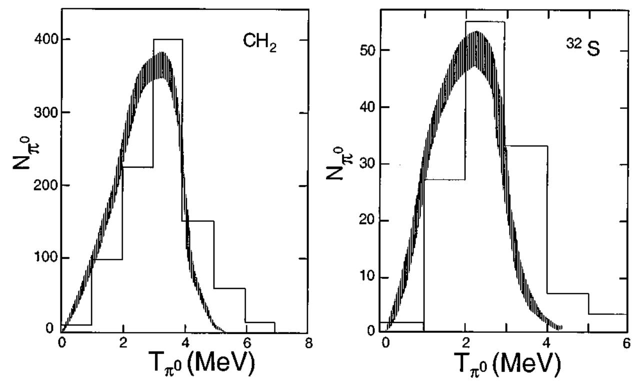

FIG. 2. Histograms showing the number of π^0 spectrometer counts vs π^0 kinetic energy for targets of CH_2 and ^{32}S. The results of the Monte Carlo simulation (shaded area) are also shown.

Typical histograms showing N_{π^0} vs π^0 kinetic energy are shown in Fig. 2. Results of Monte Carlo calculations of the energy spectrum are shown for comparison. Such histograms were obtained for each data run. For these Monte Carlo calculations, Gaussian distributions were used and isotropic π^0 emission was assumed. The BR of (π^-,π^0) was calculated from the relation

$$\mathrm{BR}=\sum_{i=1}^{n}\frac{N_{\pi_i^0}}{N_{\pi^-}\epsilon_{\mathrm{tot}}\Delta\Omega}4\pi, \tag{1}$$

where i is the number of bins in the histogram, $N_{\pi_i^0}$ the number of counts per bin, N_{π^-} the number of stopped π^- in the target, ϵ_{tot} the total efficiency, and $\Delta\Omega$ the geometrical solid angle. That angle was calculated with a Monte Carlo program, with errors ranging from 2 to 8%. The errors contributing to ϵ_{tot} were about 2%.

Comparison of the experimental histograms with the Monte Carlo results allows an estimate of the contribution to the π^0 yield from incompletely stopped π^-'s in the target. In the Monte Carlo calculation, the π^-'s are assumed to be completely stopped, so that the calculated distribution is centered around a π^0 kinetic energy determined by the reaction Q value (Table I). The experimental distributions are shifted to higher energies; the highest detected π^0 energy is about 4 MeV above the Monte Carlo centroid, which is consistent with the energy of the π^-'s when they entered the target. The BR for (π^-,π^0) determined in this experiment is, therefore, the BR for incident energies between 0 and 4 MeV. The difficulty of excluding events produced by incompletely stopped pions in the target is systematic and was present also in all previous BR determinations near threshold.

Our results are shown in Table I [7]. The BR(π^-,π^0) for CH_2 has been previously measured in the course of determinations of the pion capture rate,

$$W=\mathrm{BR}(\pi^-,\pi^0)+\mathrm{BR}(\pi^-,\gamma).$$

Experiments at CERN [8], Nevis [9], and Dubna [10] yielded BR(π^-,π^0) values equal to $(850\pm70)\times10^{-5}$, $(1070\pm110)\times10^{-5}$, and $(640\pm100)\times10^{-5}$, respectively. The Dubna value was obtained by us from their value for W and from the Panofsky ratio (PR) value [11]

$$\mathrm{PR}=\mathrm{BR}(\pi^-,\pi^0)/\mathrm{BR}(\pi^-,\gamma)=1.546\pm0.009. \qquad (2)$$

Clearly, these earlier results are incompatible with one another. Our result, $(869\pm78)\times10^{-5}$, favors the CERN result. The pion capture rate W for CH_2, calculated from our measured BR and the PR value, Eq. (2), is $(14.3\pm1.3)\times10^{-3}$.

The Q values shown in Table I were calculated from the equation

$$Q=m_{\pi^-}+m_A+E_n-(m_{\pi^0}+m_B), \qquad (3)$$

where E_n is the negative energy of the π^- bound in an atomic orbit having principal quantum number n and m_A and m_B are, respectively, the mass of the target and product nuclei. The most populated pionic orbit in the nuclei studied has $n=3$. The Q value for CH_2 is that for the elementary reaction $p(\pi^-_{\mathrm{stop}},\pi^0)n$ because the reaction on ^{12}C is energetically forbidden. Indeed, we did not observe any SCX events for ^{12}C.

To understand qualitatively our other results, it suffices to examine charge exchanges due only to stopped pions which, as can be seen from Fig. 2, represent the majority of the events. Before undergoing a charge exchange, the π^- is captured into an atomic orbit having an orbital angular momentum L. Because the produced π^0 has a very low energy, the final pion-nucleus system is in an s-wave state, $l=0$. Consequently, the angular momentum transferred to the nucleus is $\Delta L=L-l=L$.

We have carried out a cascade calculation to estimate the probabilities of pion capture into different atomic orbits in the nuclei ^{27}Al, ^{31}P, and ^{32}S. Using the set-B parameters of Tauscher [12] and the set-($a2$) parameters of Seki and Masutani [13] for the pion-nucleus optical potential, we found the capture probabilities in the $1s$, $2p$, and $3d$ orbits to be about 6%, 91.5%, and 2.5%, respectively, in ^{27}Al and about 3%, 90%, and 7%, respectively, in both ^{31}P and ^{32}S. Hence, in ^{31}P and ^{32}S there are about half as many pions captured into the $1s$ orbit as into the $3d$ orbit. The situation is, however, reversed in ^{27}Al. Since the $\Delta L=1$ transition will lead to J^- nuclear states and since there are no low-lying negative-parity states in this nucleus, the pions captured into the $2p$ atomic orbit do not contribute to threshold SCX. On the other hand, the pions captured into the $1s$ and $3d$ orbits have, respectively, angular momenta $L=0$ and 2 and will lead to positive-parity states via $\Delta L=0$ and 2 transitions. The spin and parity of ^{27}Al is $J^\pi=\frac{5}{2}^+$. The $\Delta L=0$ transition, arising from pions captured into the $1s$ atomic orbit, leads to $\frac{5}{2}^+$ states in ^{27}Mg. Because the $\frac{5}{2}^+$ states have excitation energies higher than the reaction Q value (1.33 MeV), the $\Delta L=0$ transition is energetically forbidden. The $\Delta L=2$ transition can lead to $\frac{1}{2}^+$ (g.s.) and $\frac{3+}{2}$ (0.98 MeV) states in ^{27}Mg. Shell-model calculations indicate that only the transition to the $\frac{3}{2}^+$ state has an appreciable matrix element. Since only the pions captured into the $3d$ atomic orbit can contribute to threshold SCX in ^{27}Al while pions captured into both the $1s$ and $3d$ orbits can contribute to threshold SCX in ^{31}P and ^{32}S, the effective number of pions captured by ^{27}Al is only a fraction of those captured by ^{31}P and ^{32}S. This fraction can be calculated from the ratio of the corresponding capture rates and is given by $x\equiv2.5\%/(3\%+7\%)=0.25$. We have also used the other sets of pion-nucleus optical potential parameters in Refs. [12] and [13] and have found that for those potentials $x=0.2$–0.35. In other words, with respect to ^{31}P, the small reaction Q value for ^{27}Al reduces, in the main, the effectiveness of pion SCX by a factor of 4. Our measured data (Table I) show that SCX in ^{27}Al is about a factor of 10 smaller than in ^{31}P. A similar small BR for ^{27}Al has also been observed in a previous experiment [3].

Thus we can understand why the SCX yield in ^{27}Al is much smaller than in ^{31}P. A Clearly, quantitative microscopic theoretical investigations are needed in the future in order to understand this additional factor of 2 reduction. It can be expected, for instance, that a difference between the effective isovector pion-nucleon interactions and the proton density distribution tails in ^{31}P and ^{27}Al might account for this factor of 2. To this end, we would like to recall that one of our motivations of the present investigation is indeed to obtain data to facilitate such theoretical analyses.

The J^π of ^{31}P is $\frac{1}{2}^+$. Given the reaction Q value of 2.51 MeV, the only state in ^{31}Si that can be reached by a $\Delta L=0$ transition is $\frac{1}{2}^+$ (0.75 MeV). Those that can be reached by a $\Delta L=2$ transition are $\frac{3}{2}^+$ (g.s.), $\frac{5}{2}^+$ (1.69 MeV), and $\frac{3}{2}^+$ (2.32 MeV). Shell-model calculations indicate that only the $^{31}\mathrm{P}\rightarrow{}^{31}\mathrm{Si}$(g.s.) transition has a large one-body transition matrix element. The J^π of ^{32}S is 0^+. The $\Delta L=0$ transition leads to the 0^+ (0.51 MeV) state and the $\Delta L=2$ transition to 2^+ states in ^{32}P. There are two low-lying 2^+ states that can be reached by the available reaction Q value (2.28 MeV), 2^+ (0.078 Mev), and 2^+ (1.32 MeV). Shell-model calculations show that the matrix element for the transition to a 0^+ state is very small, while the matrix elements for transitions to both 2^+ states are large and equally important. Consequently, the number of favored transitions in ^{32}S is twice that in ^{31}P. In addition, the isospin coefficient for SCX in ^{31}P is about half of that in ^{32}S, reflecting the fact that in ^{31}P there is only one proton in the dominant $(2s_{1/2})$ wave-function component on which SCX takes place, while in ^{32}S there are two. This agrees with our result that the BR for ^{32}S is 4 times larger than that for ^{31}P.

The BR observed for ^{45}Sc can be understood in a similar manner. We note that there is only one least bound proton in ^{45}Sc and that for all possible transitions to low-lying states in ^{45}Ca only the $^{45}\mathrm{Sc}\rightarrow{}^{45}\mathrm{Ca}$(g.s.) matrix element is important. Thus the BR for ^{45}Sc is expected to be similar to the BR for ^{31}P, which is indeed the case.

Finally, ^{115}In has its least bound proton in the $1g_{9/2}$ orbit. The reaction Q value enables the produced neutron to occupy states mainly in the $3s_{1/2}$ and $1h_{11/2}$ regions in the final nucleus. Because the spatial parts of these states are nearly orthogonal to that of the initial proton state, the BR for ^{115}In is expected to be very small, which agrees with our experimental result.

In summary, we have experimentally determined the branching ratios for single charge exchange induced by negative pions close to threshold in CH_2, ^{31}P, ^{32}S, and ^{45}Sc, and we have established upper limits for ^{27}Al and ^{115}In. We have found our results to be in qualitative agreement with considerations based on the shell-model structure of the target and product nuclei and with previous work where comparisons are possible. Theoretical calculations with which our results can be compared are called for. They are expected to lead to values of the parameters for the isovector part of the pion-nucleon optical potential at very low energies.

This work was supported in part by the National Science Foundation and the Department of Energy. We thank Dr. Alex Brown for sending us the results of his shell-model calculations. We also thank Prof. Ryoichi Seki for discussions relating to pionic atoms and Dr. C. J. Morris for discussions of experimental results.

[1] V. I. Petrukhin and Yu. D. Prokoshkin, Nucl. Phys. **54**, 414 (1964).

[2] R. MacDonald, D. S. Beder, D. Berghofer, M. D. Hasinoff, D. F. Measday, M. Salomon, J. Spuller, and T. Suzuki, Phys. Rev. Lett. **38**, 746 (1977).

[3] B. Bassalleck, F. Corriveau, M. D. Hasinoff, T. Marks, D. F. Measday, J.-M. Poutissou, and M. Salomon, Nucl. Phys. **A362**, 445 (1981).

[4] LAMPF Users Handbook-LEP section, LASL Report No. MP-DO-3-UHB, 1980.

[5] H. W. Baer *et al.*, Nucl. Instrum. Methods **180**, 445 (1981).

[6] G. W. Butler, B. J. Dropesky, C. J. Orth, R. Green, R. G. Korteling, and K. Y. Lam, Phys. Rev. C **26**, 1737 (1982).

[7] Preliminary results were published as follows: H. S. Plendl *et al.*, in Proceedings of the 6th International Conference on Nuclear Reaction Mechanisms, Varenna, 1991 (Ricerca Scientifica ed Educazione Permanente, Supplemento No. 84, Milano, 1991), p. 712; and in Proceedings of the International Conference on Meson-Nucleus Interactions, Cracow, 1993 [Acta Phys. Pol. B **24**, 1649 (1993)].

[8] M. Chabre, P. Depommier, J. Heintze, and V. Soergel, Phys. Lett. **5**, 67 (1963).

[9] D. Bartlett, S. Devons, S. L. Meyer, and J. L. Rosen, Phys. Rev. **136**, B1452 (1964).

[10] A. F. Dunaitsev, V. I. Petrukhin, and Yu. D. Prokoshkin, Nuovo Cimento **34**, 521 (1964).

[11] J. Spuller, D. Berghofer, M. D. Hasinoff, R. MacDonald, D. F. Measday, M. Salomon, T. Suzuki, J.-M. Poutissou, R. Poutissou, and J. K. P. Lee, Phys. Lett. **67B**, 479 (1977).

[12] L. Tauscher, in *Physics of Exotic Atoms*, edited by G. Fiorentini and G. Torelli (INFN, Frascati, 1977), p. 145. See also Torleif Ericson and Wolfram Weise, *Pions and Nuclei* (Clarendon, Oxford, 1988), p. 206, Table 6.2.

[13] R. Seki and K. Masutani, Phys. Rev. C **27**, 2799 (1983).